Securing the Deep Fraud Detector in Large-Scale E-Commerce Platform via Adversarial Machine Learning Approach

Qingyu Guo
Nanyang Technological University
qyguo@ntu.edu.sg

Zhao Li
Alibaba Group
lizhao.lz@alibaba-inc.com

Bo An
Nanyang Technological University
boan@ntu.edu.sg

Pengrui Hui, Jiaming Huang
Alibaba Group
{pengrui.hpr,jimmy.hjm}@alibaba-inc.com

Long Zhang
Alibaba Group
james.zl@alibaba-inc.com

Mengchen Zhao
Nanyang Technological University
zhao0204@ntu.edu.sg

ABSTRACT

Fraud transactions are one of the major threats faced by online e-commerce platforms. Recently, deep learning based classifiers have been deployed to detect fraud transactions. Inspired by findings on adversarial examples, this paper is the first to analyze the vulnerability of deep fraud detector to slight perturbations on input transactions, which is very challenging since the sparsity and discretization of transaction data result in a non-convex discrete optimization. Inspired by the iterative Fast Gradient Sign Method (FGSM) for the L_∞ attack, we first propose the *Iterative Fast Coordinate Method (IFCM)* for discrete L_1 and L_2 attacks which is efficient to generate large amounts of instances with satisfactory effectiveness. We then provide two novel attack algorithms to solve the discrete optimization. The first one is the *Augmented Iterative Search (AIS)* algorithm, which repeatedly searches for effective "simple" perturbation. The second one is called the *Rounded Relaxation with Reparameterization (R3)*, which rounds the solution obtained by solving a relaxed and unconstrained optimization problem with reparameterization tricks. Finally, we conduct extensive experimental evaluation on the deployed fraud detector in TaoBao, one of the largest e-commerce platforms in the world, with millions of real-world transactions. Results show that (i) The deployed detector is highly vulnerable to attacks as the average precision is decreased from nearly 90% to as low as 20% with little perturbations; (ii) Our proposed attacks significantly outperform the adaptions of the state-of-the-art attacks. (iii) The model trained with an adversarial training process is significantly robust against attacks and performs well on the unperturbed data.

CCS CONCEPTS

• **Information systems** → Adversarial retrieval.

KEYWORDS

Online Shopping; Fraud Detection; Adversarial Machine Learning

This paper is published under the Creative Commons Attribution 4.0 International (CC-BY 4.0) license. Authors reserve their rights to disseminate the work on their personal and corporate Web sites with the appropriate attribution.
WWW '19, May 13–17, 2019, San Francisco, CA, USA
© 2019 IW3C2 (International World Wide Web Conference Committee), published under Creative Commons CC-BY 4.0 License.
ACM ISBN 978-1-4503-6674-8/19/05.
https://doi.org/10.1145/3308558.3313533

ACM Reference Format:
Qingyu Guo, Zhao Li, Bo An, Pengrui Hui, Jiaming Huang, Long Zhang, and Mengchen Zhao. 2019. Securing the Deep Fraud Detector in Large-Scale E-Commerce Platform via Adversarial Machine Learning Approach. In *Proceedings of the 2019 World Wide Web Conference (WWW'19), May 13–17, 2019, San Francisco, CA, USA.* ACM, New York, NY, USA, 11 pages. https://doi.org/10.1145/3308558.3313533

1 INTRODUCTION

With the rapid growth of information technologies, e-commerce has become prevalent nowadays. Large e-commerce platforms serve billions of users and connect them to factories, stores and third-party merchants with numerous products available. The big success of e-commerce also motivates the emergence of fraud transactions to illegally promote items and stores. In order to increase sales, fraudulent sellers turn to third-party malicious service platforms where they can hire human labors to create fake purchases and visits [26, 29, 33], and thus provide a fake impression that the target item is popular. This results in much higher rankings of the items from fraudulent sellers, and causes huge losses to the platforms as it hurts the user experience. Online fraud activities have caused a loss in billions of dollars[1], and it is reported that just in China, the online fraudulent industries involve over 1.6 million human labors and create billions of dollars of illegal incomes[2].

Fraud detection is critical to the development of e-commerce platforms. Recently, with billions of transaction data available, deep learning based models are proposed and deployed to detect fraud transactions on a real-time basis [6, 32, 34]. Inspired by recent findings in the domain of computer vision that deep learning based image classifiers could be fooled by imperceptible noises during test phases [27], we are interested in analyzing the vulnerability of deep fraud detector to slight perturbations on input data. This study has a high practical value for e-commerce platforms as the existence of such adversarial perturbations could indicate the risk of deploying deep fraud detectors. As shown in our motivating example, fraudulent sellers and malicious service providers are able to exploit such risks to bypass the detector with little costs.

In this paper, we aim to investigate the vulnerability of a deployed deep fraud detector being fooled by slight and feasible perturbations. However, the e-commerce domain is different from the computer vision area, since the transaction data are mostly discrete and sparse.

[1] https://www.signifyd.com/blog/2017/10/26/ecommerce-fraud-eight-industries/
[2] http://cn.chinadaily.com.cn/2015-11/05/content_22379527.htm

Few works considering discrete adversarial perturbations either propose a straightforward extension of the existing Fast Gradient Method [9], or take into account only the L_∞ attack [2], while they cannot handle more complex L_1 and L_2 attacks, which are of higher practical interests in our problem.

This paper makes the following contributions.

- First, inspired by the Fast Gradient Sign Method (FGSM), to handle the L_1 and L_2 norm bound constraints, we propose the Iterative Fast Coordinate Method (IFCM) which repeatedly conducts a one-unit descent on a single coordinate. IFCM can efficiently generate a large amount of adversarial perturbations with satisfactory effectiveness and is used in our proposed adversarial training process.
- Second, to address the discrete optimization for adversarial perturbations, we provide two novel attacks. The first attack is called the *Augmented Iterative Search (AIS)*. In each iteration, AIS proceeds to search for "simple" perturbations with one-unit descents on at most two coordinates. AIS also augments the searching process by restricting the space of two-coordinate perturbations based on the *Value of Perturbation (VoP)*. The second attack is called the *Rounded Relaxation with Reparameterization (R3)*, which is an optimization-based attack. R3 first relaxes the discrete optimization with reparameterization trick and rounds the continuous solution to obtain a discrete perturbation.
- Third, we conduct extensive experimental evaluations on the deployed fraud detector from TaoBao, one of the largest e-commerce platforms in the world, with millions of real-world transactions. The experimental results show that (i) The deployed fraud detector is threatened by the crafted adversarial perturbations. Our AIS and R3 attacks successfully decrease the detector's average precision from nearly 90% to as low as 20% with little perturbations. (ii) Our proposed AIS and R3 attacks significantly outperform adaptations of several state-of-the-art attacks, including the C&W attack [4], the Logit-Space attack [2], and the EAD attack [5]. (iii) We propose an adversarial training process with adversarial examples generated by the IFCM. Results show that the robustness of the detection model is significantly improved as we achieve an average precision above 85.9% under all tested attacks. Meanwhile, the average precision on the unperturbed data remains nearly 90%.

2 RELATED WORK

In this section, we review the related works in crafting adversarial examples to attack DNN models and various defense techniques.

2.1 Attacks on DNNs

FGSM [8] and its variant R+FGSM [28] are single step attacks, which perturb the input towards the gradient direction of the loss function. The extensions of FGSM iteratively perform single step attacks with smaller step size, such as BIM [13] and PGD [15]. Other iterative attacks include DeepFool [17], which approximates the decision boundary near the target instance with the linear hyperplane, and UAP [16] to produce a single perturbation which is capable of attacking multiple images. FGSM and R+FGSM are further extended to perturb towards the direction which maximizes the confidence score on the least likely labels for the target image [8, 28].

Besides gradient directional methods, Papernot et al. [21] propose the JSMA attack which uses the Jacobian matrix to get the salient map and modifies the features with high significance to confuse the classifier. C&W attack [3] relaxes the hard constraint on the distortion, and adds a penalty on the L_p norm ($p \in \{0, 2, \infty\}$) of perturbation. EAD [5] improves the transferability of adversarial examples through elastic-net regularization. Several works study the adversarial examples to evade DNN models in real-world applications, including the face recognition system [25], objection detection [11], and malware detection [9].

Most of the works focus on image recognition tasks and consider only continuous perturbations. While Grosse et al. consider the binary input [9] and adapt the fast gradient algorithms to solve their problem in a similar way as our IFCM$_1$, they only consider the L_1 attack. Buckman et al. propose the Gumbel-softmax trick to approximate the one-hot encoding of the discrete feature. However, their attack is suitable for L_∞ distortion bound and fails to consider the constraints that correlate the input features such as L_1 and L_2 norm constraints in our problem.

Our R3 attack is inspired by the optimization-based L_2 attacks [4, 5, 27]. These attacks all handle the L_2 norm constraint by imposing a penalty in the objective function and conducting a binary search to find a suitable constant coefficient of penalty term. This is a reasonable way to find the minimal distortion to successfully craft an adversarial example. However, in our problem, we are asked to find the most effective adversarial instance given the allowed distortion. While one could conduct a binary search to find the suitable constant coefficient that the distortion constraint is satisfied, the neural networks are non-convex in general and thus the binary search could be unstable to always generate a distortion satisfying the given constraint [27]. Our R3 attack utilizes the reparameterization trick to transform the constrained optimization to an equivalent unconstrained problem for which the solution always satisfies the distortion bound.

2.2 Defenses

There are several defense measures to improve the robustness of deep learning based classifiers, such as the defensive distillation [20, 22], which adopts the distillation technique [10] to retrain the same network with the confidence score outputted by the original model as the soft label, feature squeezing [30], detection approaches for adversarial instances [4], and adversarial training [8], a general process based on robust optimization that augments the training data with adversarial examples [8, 15, 35]. Some recent works propose to regularize or mask the gradient of the loss function with respect to inputs [24]. Almost all defenses are shown to be effective only for some attacks [31].

Recently, Athalye et al. pointed out that the defenses based on obfuscated gradients are threatened by their characteristic behaviors which can be exploited to design attacks circumventing them [1]. It is believed that adversarial training does not cause obfuscated gradient [1]. Thus, in this paper, we use adversarial training to achieve robust fraud detection and our experimental evaluation verifies the effectiveness of the strengthened detector.

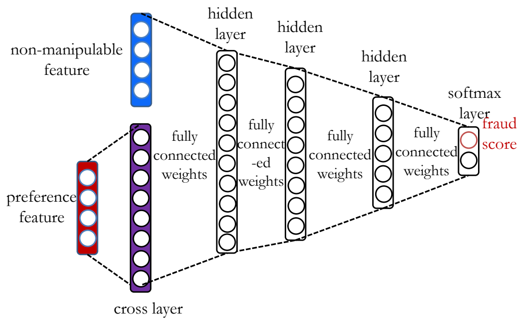

Figure 1: Abstracted architecture of deep fraud detector

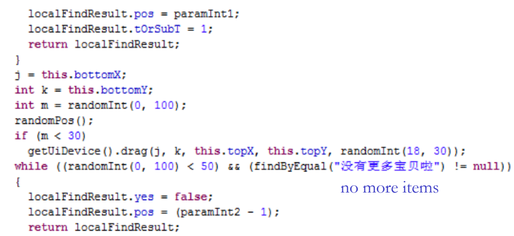

```
    localFindResult.pos = paramInt1;
    localFindResult.tOrSubT = 1;
    return localFindResult;
  }
  j = this.bottomX;
  int k = this.bottomY;
  int m = randomInt(0, 100);
  randomPos();
  if (m < 30)
    getUiDevice().drag(j, k, this.topX, this.topY, randomInt(18, 30));
  while ((randomInt(0, 100) < 50) && (findByEqual("没有更多宝贝啦") != null))
  {
    localFindResult.yes = false;
    localFindResult.pos = (paramInt2 - 1);
    return localFindResult;
```


Figure 2: A piece of a fraudulent automatic script

3 DEEP FRAUD DETECTION AND ATTACKS

In this section, we first briefly introduce the deep learning model for fraud detection which is used by one of the largest e-commerce platforms in the world. We then present concrete examples to show the possible attacks by malicious sellers and service providers.

3.1 Deep Fraud Detection

Figure 1 shows the architecture of deep neural networks in deployed fraud detection system of TaoBao. The goal of the detector is to predict whether an online transaction is fraudulent. Each input transaction is represented as a feature vector $\mathbf{x}$ which concatenates two classes of features. The first is non-manipulable features, such as scores obtained with label propagation on the user-item transaction graph, to measure the offline maliciousness based on past records. Other non-manipulable features are prices[3]. In this paper, we focus on manipulatable features whose adjustment could have a significant effect on the detector's prediction. Without causing any confusion, we denote a transaction by a vector of only perturbable features. In the context of the investigated fraud detection, the perturbable features are those characterizing the user's preference, called *preference features*, defined as follows.

Let C be the set of all item categories, and $n = |C|$. A preference feature vector is represented by $\mathbf{x} \in \mathbb{N}^n$ with x_i denoting the number of records that the user interacts with items in the i-th category of C in a past period, normally 30 days. Such records include adding an item to the shopping cart, adding an item to "favorite", and so on. $\mathbf{x}$ represents the user's global interest in online shopping. Fraudulent buyers tend to show different preference patterns compared with benign users. Each transaction instance $\mathbf{x}$ is associated with a label $y \in \{0, 1\}$, such that $y = 1$ if the transaction is fraudulent and $y = 0$ otherwise.

All features are first normalized to be within $[0, 1]^n$ with a "smooth" normalization function to tackle the extreme values. Here, the feature value $\mathbf{x}$ is normalized to be $\frac{\log(\mathbf{x}+1)}{\log M}$ (element-wise) where M is the largest number of interactions observed in training data. The normalized preference features are passed to a cross layer [14] at first to exploit the interactions between different categories. The output of the cross layer is concatenated with non-manipulable features. The aggregated feature vector goes to a multi-layer feed-forward neural network, where each hidden-layer consists of rectified linear units as hidden neurons [18]:

$$relu(x) = \max(0, x).$$

The output of the last hidden-layer $\mathbf{z} \in \mathbb{R}^2$, called the *logit*, is then passed to a softmax layer to produce the confidence score on the transaction $\mathbf{x}$ being fraudulent

$$f^{\mathbf{w}}(\mathbf{x}) = \frac{e^{z_1}}{e^{z_0} + e^{z_1}},$$

where $\mathbf{w}$ denotes the parameters of the model, including the weights and biases on hidden neurons. The model is trained over a large-scale data set $\mathcal{D} = \{\mathbf{x}^i, y^i\}_{i=1}^N$ by minimizing the regularized total loss function $L^{\mathbf{w}}(\mathbf{x}, y)$ over $\mathcal{D}$

$$\min_{\mathbf{w}} \mathop{\mathbb{E}}_{(\mathbf{x}, y) \sim \mathcal{D}} [L^{\mathbf{w}}(\mathbf{x}, y)] + \lambda \|\mathbf{w}\|^2, \tag{1}$$

where λ is the regularization coefficient. The commonly used loss function in classification tasks is the cross-entropy loss

$$L^{\mathbf{w}}(\mathbf{x}, y) = -\mathbb{1}_{\{y=1\}} \log f^{\mathbf{w}}(\mathbf{x}) - \mathbb{1}_{\{y=0\}} \log (1 - f^{\mathbf{w}}(\mathbf{x})),$$

and the stochastic gradient descent is widely applied to optimize the parameter $\mathbf{w}$ [7, 23].

3.2 Attacks to Fraud Detector

With billions of customers served on e-commerce platforms, the profit from fraud transactions could be huge for malicious sellers as they significantly promote the rankings of target items. Driven by the huge profit, a lot of malicious service platforms provide sophisticated tactics to bypass the strict detection and conduct fraud transactions. One common tactic is to mimic benign users' behavior such as using automatic visit script to visit different items before purchasing the target item, and hiring human labors to chat with the merchants before making a transaction. Figure 2 shows an example of automatic script to bypass the fraud detection, which is a piece of Java code as part of a mobile malicious service App which creates random perturbation to a target transaction such as dragging and browsing to behave like humans, intentionally visiting items from some categories, etc. According to domain experts, malicious platforms can create around 200,000 visits in per day and promote over 1000 items from malicious sellers. Since we verify that the vulnerability to slight perturbations exists for a fraud detector, the malicious platforms could exploit those threats to adapt the fraud transaction data in order to bypass the detection.

[3]Prices are hard to perturb in practice and the empirical study shows that slight perturbations on prices cause negligible changes.

Formally, let δ be the vector of perturbation on fraud instance $\mathbf{x}$ where δ_i is the amount of changes on x_i, and δ is discrete, i.e., $\delta \in \mathbb{Z}^n$. Assume $\delta \geq \mathbf{0}$ since it is more practical for realistic adversaries to add additional records of interactions via measures such as aforementioned automatic scripts[4]. In the domain of computer vision, the adversarial perturbations need to satisfy constraints that the perturbations are small enough, so that the ground truths of the adversarial instances remain the same as the original ones [8]. We also impose similar restrictions on δ, in order to capture the *feasibility* of perturbations in the sense that adversaries can conduct the perturbation with little effort. Such restrictions are expressed by the L_p norm bound on perturbations, and the common choices of p are $\{0, 1, 2, \infty\}$. Thus, the set of feasible δ bounded by L_p norm is defined as follows:

$$\Delta_q^p \coloneqq \{\delta \mid \delta \in \mathbb{Z}^n, \|\delta\|_p \leq q, \delta \geq \mathbf{0}\}, \tag{2}$$

where q is the maximal distortion in L_p norm, and

$$\|\delta\|_0 = \sum_{i=1}^{n} \mathbb{1}_{\{\delta_i > 0\}}, \qquad \|\delta\|_1 = \sum_{i=1}^{n} |\delta_i|,$$

$$\|\delta\|_2 = \sqrt{\sum_{i=1}^{n} \delta_i^2}, \qquad \|\delta\|_\infty = \max_i |\delta_i|.$$

We focus on attacks bounded by L_1 and L_2 norms, which are suitable to describe realistic perturbations on the discrete and sparse preference features. L_0 attack is not practical as it allows the adversary to add infinitely many records on one category. L_∞ attack is not reasonable as the preference features are sparse in the sense that interactions on only few categories are recorded. Thus, even an adversarial perturbation with L_∞ norm of 1 violates the sparse nature of preference features.

For a suitable distortion metric L_p, our objective is defined as follows. For a deep fraud detector with model parameter $\mathbf{w}$, given a fraud transaction instance $\mathbf{x}$ in testing or deploying phase, we aim to find the adversarial example, an instance $\mathbf{x}^{adv}$ crafted with a feasible perturbation $\delta \in \Delta_q^p$, i.e., $\mathbf{x}^{adv} = \mathbf{x} + \delta$, to maximally decrease the fraudulent score on $\mathbf{x}^{adv}$. This can be done by solving the following optimization problem:

$$\min_{\delta \in \Delta_q^p} \quad f^{\mathbf{w}}(\mathbf{x} + \delta) \tag{3}$$

In the following sections, we present our three novel L_1 and L_2 attack algorithms. We first provide an *Iterative Fast Coordinate Method (IFCM)* which is efficient enough to generate a large number of adversarial examples with satisfactory attacking effectiveness. Therefore, IFCM is used in the defense measure of adversarial training. To evaluate the robustness of the detector more accurately, we provide two stronger attacks. One is the search-based attack called *Augmented Iterative Search (AIS)*, and the second one is optimization-based attack called *Rounded Relaxation with Reparameterization (R3)*. Though AIS and R3 cannot generate millions of adversarial examples for adversarial training, their scalability is sufficient to evaluate the robustness of the model, and both algorithms outperform the adaption of the state-of-the-art methods significantly in attacking effectiveness. Empirical evaluation shows that with adversarial training on samples generated by IFCM, the model is significantly more robust against stronger attacks such as AIS and R3.

[4]Note that, our attacks can be easily adapted to allow negative perturbations.

4 FAST ATTACK: IFCM

In this section, we propose a fast attack algorithm called *Iterative Fast Coordinate Method* (IFCM), which is inspired by the iterative gradient sign method [13]. Given the sparsity and discretilization of input data, IFCM conducts multiple gradient descents, each with step size 1 along a single coordinate. The descending coordinate is selected in different ways when generating L_1 and L_2 attacks respectively. In IFCM for L_1 attack (IFCM$_1$), the coordinate with the smallest partial derivative is chosen. While in IFCM for L_2 attack (IFCM$_2$), the selection of descending coordinate considers not only the value of partial derivative along that coordinate, but also the increment of L_2 norm caused by one unit descent along the coordinate. Thus, following the greedy algorithm for the knapsack problem, IFCM$_2$ selects the coordinate with the highest *Value of Perturbation* (VoP) which is defined later. The two variants of IFCM are illustrated as follows.

4.1 IFCM$_1$

Algorithm 1: Iterative Fast Coordinate Method for L_1 attack (IFCM$_1$)

input : Fraud instance $\mathbf{x}$, q, detection model parameter $\mathbf{w}$
output: Adversarial example $\mathbf{x}^{adv}$ with L_1 norm bounded distortion

1 $\mathbf{x}^{adv} \leftarrow \mathbf{x}, \delta \leftarrow \mathbf{0}_n$;
2 **while** $\sum_{i=1}^{n} \delta_i < q$ **do**
3   Compute the gradient $\nabla_{\mathbf{x}} f^{\mathbf{w}}(\mathbf{x}^{adv})$ with back-propagation;
4     $i_{min} = \arg\min_i \frac{\partial f^{\mathbf{w}}(\mathbf{x}^{adv})}{\partial x_i}$;
5   **if** $\frac{\partial f^{\mathbf{w}}(\mathbf{x}^{adv})}{\partial x_{i_{min}}} > 0$ **then**
6   **return** $\mathbf{x}^{adv}$;
7     $x_{i_{min}}^{adv} \leftarrow x_{i_{min}}^{adv} + 1, \delta_{i_{min}} \leftarrow \delta_{i_{min}} + 1$;
8 **return** $\mathbf{x}^{adv}$.

As illustrated by Algorithm 1, at each iteration, IFCM$_1$ computes the gradient $\nabla_{\mathbf{x}} f^{\mathbf{w}}(\mathbf{x}^{adv})$ of the fraudulent score with the current adversarial example (Line 3), and selects the coordinate i_{min} with the minimal partial derivative (Line 4). If the partial derivative of $f^{\mathbf{w}}(\mathbf{x}^{adv})$ with $x_{i_{min}}$ is negative, a step of coordinate descent along the coordinate i_{min} is conducted with step size 1. Otherwise, when the gradient $\nabla_{\mathbf{x}} f^{\mathbf{w}}(\mathbf{x}^{adv})$ is positive along every coordinate, or the maximal distortion q is reached, the algorithm terminates.

4.2 IFCM$_2$

The main difference between IFCM$_2$ and IFCM$_1$ lies in the choice of descending coordinate. IFCM$_1$ selects the coordinate by comparing the partial derivative, while the coordinate chosen in IFCM$_2$ is decided by *Value of Perturbation* (VoP). VoP is inspired by the greedy algorithm for knapsack problem. For each coordinate i, a unit descent on such coordinate decreases the fraudulent score $f^{\mathbf{x}^{adv}}$ by

Algorithm 2: Iterative Fast Coordinate Method for L_2 attack (IFCM$_2$)

input : Fraud instance $\mathbf{x}$, q, detection model parameter $\mathbf{w}$
output : Adversarial example $\mathbf{x}^{adv}$ with L_1 norm bounded distortion

$\mathbf{x}^{adv} \leftarrow \mathbf{x}, \delta \leftarrow \mathbf{0}_n$;
while $\sqrt{\sum_{i=1}^{n} \delta_i^2} < q$ **do**
  Compute the gradient $\nabla_{\mathbf{x}} f^{\mathbf{w}}(\mathbf{x}^{adv})$ with back-propagation;
  Compute VoP_i for $i \in [n]$;
  $i_{max} = \arg\max_i VoP_i$;
  if $VoP_{i_{max}} \leq 0$ **then**
    return $\mathbf{x}^{adv}$;
  $x^{adv}_{i_{max}} \leftarrow x^{adv}_{i_{max}} + 1, \delta_{i_{max}} \leftarrow \delta_{i_{max}} + 1$;
return $\mathbf{x}^{adv}$.

an estimated amount of $-\frac{\partial f^{\mathbf{w}}(\mathbf{x}^{adv})}{\partial x_i}$ (the *value*), and increases the L_2 norm of current perturbation δ by $\sqrt{\|\delta\|_2^2 + 2\delta_i + 1} - \|\delta\|_2$ (the *weight*). VoP_i is defined as the estimated decrease on the fraudulent score per unit increase of L_2 norm via increasing δ_i

$$VoP_i = \begin{cases} \frac{-\frac{\partial f^{\mathbf{w}}(\mathbf{x}^{adv})}{\partial x_i}}{\sqrt{\|\delta\|_2^2 + 2\delta_i + 1} - \|\delta\|_2} & \text{if } \sqrt{\|\delta\|_2^2 + 2\delta_i + 1} \leq q \\ -\infty & \text{otherwise.} \end{cases}$$

5 SEARCH-BASED ATTACK: AIS

In order to further evaluate the vulnerability of deep fraud detector to adversarial perturbation, we propose an attack method called *Augmented Iterative Search* (AIS) which shows superior performance in fooling the detector and outperforms all benchmarks significantly in our experimental evaluation. Since the size of perturbation space is a combinatorial number, for example, $|\Delta_q^1| = C_{n+q-1}^{q}$, the exhaustive search is intractable. Thus, AIS repeatedly searches for a "simple" perturbation which brings the largest decrease on the objective value of optimization (3) and accumulates those "simple" perturbations to form the final solution. The simplest perturbation perturbs only one coordinate with a single unit, which is the one with L_1 norm of 1, termed "single-unit" perturbation. AIS goes further by taking into account the perturbations which perturb two entries with non-zero changes, one with 1 and one with -1[5], termed "tuple-unit" perturbations. However, the number of feasible tuple-unit perturbations is of quadratic order $O(n^2)$ with n, which makes it impractical to exhaustively search all of them. Thus, AIS augments the search process of the tuple-unit perturbations by restricting the space of such perturbations, as we explain later.

5.1 AIS$_1$

Similarly as IFCM, we implement two variants of AIS, AIS$_1$ and AIS$_2$, for L_1 and L_2 attacks respectively. AIS$_1$ is illustrated in Algorithm 3. δ^t denotes the accumulative perturbations until iteration t and $\delta^0 = \mathbf{0}$. At each iteration t, the set of all single-unit perturbations is denoted by $\Delta_t^- \cup \Delta_t^+$ where Δ_t^- contains the single-unit perturbations which have value -1 on the only non-zero entry and the adoption of $\delta^- \in \Delta_t^-$ decreases the L_1 norm of accumulative perturbation δ^{t-1} by 1. Similarly, $\delta^+ \in \Delta_t^+$ has value 1 on the only non-zero entry.

$$\begin{aligned} \Delta_t^- &= \{\delta \in \mathbb{Z}^n \mid \|\delta\|_1 = 1, \|\delta^{t-1} + \delta\|_1 = \|\delta^{t-1}\|_1 - 1, \delta^{t-1} + \delta \geq \mathbf{0}\} \\ \Delta_t^+ &= \{\delta \in \mathbb{Z}^n \mid \|\delta\|_1 = 1, \|\delta^{t-1} + \delta\|_1 = \|\delta^{t-1}\|_1 + 1\}. \end{aligned} \tag{4}$$

The set of all tuple-unit perturbations is denoted by $\Delta_t^{\pm}$

$$\Delta_t^{\pm} = \{\delta^+ + \delta^- \mid \delta^+ \in \Delta_t^+, \delta^- \in \Delta_t^-\}$$

However, the size of $\Delta_t^{\pm}$ is $mn - m$ where m is the number of non-zero entries in δ^{t-1}, and in the worst case, $\|\Delta_t^{\pm}\|$ can be quadratic with n. To augment the search of tuple-unit perturbation, AIS$_1$ replaces $\Delta_t^{\pm}$ with its restricted subset $\tilde{\Delta}_{t,k}^{\pm}$ with much smaller size. In order to do so, we first define the value of a "simple" perturbation δ with respect to current solution $\mathbf{x}^{adv}$ as the marginal decrease on the objective value of (3) due to the adoption of δ

$$V(\mathbf{x}^{adv}, \delta) = f^{\mathbf{w}}(\mathbf{x}^{adv}) - f^{\mathbf{w}}(\mathbf{x}^{adv} + \delta)$$

The restricted set $\tilde{\Delta}_{t,k}^{\pm}$ is defined as follows

$$\tilde{\Delta}_{t,k}^{\pm} = \{\delta^+ + \delta^- \mid \delta^+ \in \tilde{\Delta}_{t,k}^+, \delta^- \in \tilde{\Delta}_{t,k}^-\} \tag{5}$$

where $\tilde{\Delta}_{t,k}^+ \subset \Delta_t^+$ and $\tilde{\Delta}_{t,k}^- \subset \Delta_t^-$ contain the top k single-unit perturbations among Δ_t^+ and Δ_t^- respectively ordered by values in the descending order. The intuition behind $\tilde{\Delta}_{t,k}^{\pm}$ is that a tuple-unit perturbation is more likely to have higher marginal decrease on $f^{\mathbf{w}}(\mathbf{x}^{adv})$ if it consists of the single-unit perturbations with high values. The size of $\tilde{\Delta}_{t,k}^{\pm}$ is of order $O(k^2)$, and the choice of k balances the scalability and solution quality.

The search operation in AIS$_1$ is as follows. Given the L_1 norm bound of distortion, a reasonable policy is to process the spaces of perturbations Δ_t^-, Δ_t^+ and $\tilde{\Delta}_{t,k}^{\pm}$ separately with different priorities. Δ_t^- is assigned the highest priority as the perturbation within it can decrease the L_1 norm of the accumulative perturbation. Thus, if there exists one single-unit perturbation $\delta^- \in \Delta_t^-$ with positive value, it is returned and added to δ^{t-1}, the accumulative perturbation so far (Lines 4–6). If Δ_t^- contains no single-unit perturbation with positive value, $\tilde{\Delta}_{t,k}^{\pm}$ is processed. Similarly, the tuple-unit perturbation $\delta^{\pm}$ with positive value is returned and δ^t is updated (Lines 8–10). Finally, if both Δ_t^- and $\tilde{\Delta}_{t,k}^{\pm}$ cannot decrease the objective $f^{\mathbf{w}}(\mathbf{w}(\mathbf{x}^{adv})$, AIS$_1$ searches for δ^+ with positive value from Δ_t^+, which increases the L_1 norm of accumulative perturbation by 1 (Lines 14–16).

5.2 AIS$_2$

The key difference between AIS$_2$ and AIS$_1$ is that, in AIS$_1$, a single-unit perturbation would always change the L_1 norm of the accumulative perturbation by 1, and the L_1 norm of the accumulative perturbation is unchanged when a tuple-unit perturbation is applied. However, this is not always the case when producing L_2 attacks. Therefore, the value of a "simple" perturbation needs to take into account not only the decrease of fraudulent score $f^{\mathbf{w}}(\mathbf{x}^{adv})$, but also the change of the L_2 norm of accumulative perturbation. Given

[5]Notice that the value of -1 does not necessarily violate the non-negative requirement on δ, which is the accumulative perturbation.

Algorithm 3: Augmented Iterative Search (AIS) for L_1 attack

input : Fraud instance $\mathbf{x}, q$, maximum iteration K,detection model parameter $\mathbf{w}$, k
output: Adversarial example $\mathbf{x}^{adv}$ with L_1 norm bounded distortion

$\mathbf{x}^{adv} \leftarrow \mathbf{x}, \delta^0 \leftarrow \mathbf{0}_n$;
for $t \leftarrow 1$ **to** K **do**
  Compute Δ_t^-, Δ_t^+ and $\tilde{\Delta}_{t,k}^{\pm}$ with (4) and (5);
  Solve $\min_{\delta \in \Delta_t^-} V(\mathbf{x}^{adv}, \delta)$ and get δ^-;
  if $V(\mathbf{x}^{adv}, \delta^-) > 0$ **then**
    $\delta^t \leftarrow \delta^{t-1} + \delta^-$, $\mathbf{x}^{adv} \leftarrow \mathbf{x}^{adv} + \delta^-$;
  else
    Solve $\min_{\delta \in \tilde{\Delta}_t^{\pm}} V(\mathbf{x}^{adv}, \delta)$ and get $\delta^{\pm}$;
    if $V(\mathbf{x}^{adv}, \delta^{\pm}) > 0$ **then**
      $\delta^t \leftarrow \delta^{t-1} + \delta^{\pm}$, $\mathbf{x}^{adv} \leftarrow \mathbf{x}^{adv} + \delta^{\pm}$;
    else
      if $\|\mathbf{x}^{adv} - \mathbf{x}\|_1 = q$ **then**
        return $\mathbf{x}^{adv}$
      Solve $\min_{\delta \in \Delta_t^+} V(\mathbf{x}^{adv}, \delta)$ and get δ^+;
      if $V(\mathbf{x}^{adv}, \delta) > 0$ **then**
        $\delta^t \leftarrow \delta^{t-1} + \delta^+$, $\mathbf{x}^{adv} \leftarrow \mathbf{x}^{adv} + \delta^+$;
      else
        return $\mathbf{x}^{adv}$;
return $\mathbf{x}^{adv}$

the current solution $\mathbf{x}^{adv}$ of optimization (3) and a feasible "simple" perturbation δ, we define the *Value of Perturbation (VoP)* as follows:

$$VoP(\mathbf{x}^{adv}, \delta) = \begin{cases} \frac{\Delta f^{\mathbf{w}}(\mathbf{x}^{adv}, \delta)}{d_2(\mathbf{x}^{adv}, \delta) + \epsilon} & \text{if } \|\mathbf{x}^{adv} + \delta\|_2 \geq \|\mathbf{x}^{adv}\|_2 \\ -d_2(\mathbf{x}^{adv}, \delta) \cdot \Delta f^{\mathbf{w}}(\mathbf{x}^{adv}, \delta) & \text{o.w.} \end{cases}$$

where ϵ is a small constant to avoid being divided by 0,

$$d_2(\mathbf{x}^{adv}, \delta) = \|\mathbf{x}^{adv} + \delta\|_2 - \|\mathbf{x}^{adv}\|_2,$$

and

$$\Delta f^{\mathbf{w}}(\mathbf{x}^{adv}, \delta) = f^{\mathbf{w}}(\mathbf{x}^{adv}) - f^{\mathbf{w}}(\mathbf{x}^{adv} + \delta),$$

Similar with AIS_1, we start from the definition of the single-unit perturbations, which form Δ_t^- and Δ_t^+. Δ_t^- is the same as defined in (4) while Δ_t^+ is a bit different, considering the L_2 norm constraint.

$$\Delta_t^+ = \{\delta \in \mathbb{Z}^n \mid \|\delta\|_1 = 1, \|\delta^{t-1} + \delta\|_1 = \|\delta^{t-1}\|_1 + 1, \|\delta^{t-1} + \delta\|_2 \leq q\}.$$

The restricted set $\tilde{\Delta}_{t,k}^{\pm}$ follows the definition in (5) where $\tilde{\Delta}_{t,k}^{+} \subset \Delta_t^+$ and $\tilde{\Delta}_{t,k}^{-} \subset \Delta_t^-$ contain the k single-unit perturbations with top-k *VoP*s among Δ_t^+ and Δ_t^- respectively. AIS_2 searches the"simple" perturbation in a way that, the perturbations which can decrease the L_2 norm of accumulative perturbation are evaluated first. For this aim, we divide $\tilde{\Delta}_{t,k}^{\pm}$ into two sets, $\tilde{\Delta}_{t,k}^{\pm,m}$ which consists of perturbations whose adoption can decrease the L_2 norm of accumulative perturbation, and $\tilde{\Delta}_{t,k}^{\pm,p}$, the complementary set of $\tilde{\Delta}_{t,k}^{\pm,m}$.

$$\tilde{\Delta}_{t,k}^{\pm,m} = \{\delta \in \tilde{\Delta}_{t,k}^{\pm} \mid \|\delta^{t-1} + \delta\|_2 < \|\delta^{t-1}\|_2\} \quad \tilde{\Delta}_{t,k}^{\pm,p} = \tilde{\Delta}_{t,k}^{\pm} \setminus \tilde{\Delta}_{t,k}^{\pm,m}.$$

Algorithm 4 illustrates the details of AIS_2. First, AIS_2 processes $\Delta_t^- \cup \tilde{\Delta}_{t,k}^{\pm,m}$, with perturbations decreasing the L_2 norm of the accumulative perturbation. If there exists one "simple" perturbation $\delta^- \in \Delta_t^- \cup \tilde{\Delta}_{t,k}^{\pm,m}$ with positive *VoP*, it is returned and added to δ^{t-1}, the accumulative perturbation so far (Lines 4–6). Otherwise, $\Delta_t^+ \cup \tilde{\Delta}_{t,k}^{\pm,p}$ is proceeded (Lines 8–10). The algorithm terminates if no "simple" perturbation within $\Delta_t^- \cup \Delta_t^+ \cup \tilde{\Delta}_{t,k}^{\pm}$ has positive *VoP* (Line 12) or the maximum iteration K is reached.

Algorithm 4: Augmented Iterative Search (AIS) for L_2 attack

input : Fraud instance $\mathbf{x}, q$, maximum iteration K,detection model parameter $\mathbf{w}$, k
output: Adversarial example $\mathbf{x}^{adv}$ with L_2 norm bounded distortion

1 $\mathbf{x}^{adv} \leftarrow \mathbf{x}, \delta^0 \leftarrow \mathbf{0}_n$;
2 **for** $t \leftarrow 1$ **to** K **do**
3   Compute Δ_t^-, Δ_t^+ and $\tilde{\Delta}_{t,k}^{\pm}$;
4   Solve $\min_{\delta \in \Delta_t^- \cup \tilde{\Delta}_{t,k}^{\pm,m}} VoP(\mathbf{x}^{adv}, \delta)$ and get δ^-;
5   **if** $VoP(\mathbf{x}^{adv}, \delta^-) > 0$ **then**
6     $\delta^t \leftarrow \delta^{t-1} + \delta^-$, $\mathbf{x}^{adv} \leftarrow \mathbf{x}^{adv} + \delta^-$;
7   **else**
8   Solve $\min_{\delta \in \Delta_t^+ \cup \tilde{\Delta}_{t,k}^{\pm,p}} VoP(\mathbf{x}^{adv}, \delta)$ and get δ^+;
9   **if** $VoP(\mathbf{x}^{adv}, \delta^+) > 0$ **then**
10      $\delta^t \leftarrow \delta^{t-1} + \delta^+$, $\mathbf{x}^{adv} \leftarrow \mathbf{x}^{adv} + \delta^+$;
11   **else**
12   **return** $\mathbf{x}^{adv}$
13 **return** $\mathbf{x}^{adv}$

6 OPTIMIZATION-BASED ATTACK: R3

In this section, we propose a novel attack framework called *Rounded Relaxation with Reparameterization (R3)*. R3 solves the following relaxed optimization problem of (3) and rounds the continuous solution to get the discrete perturbation.

$$\begin{aligned} \min_{\delta \in \mathbb{R}_{+,0}^n} \quad & f^{\mathbf{w}}(\mathbf{x} + \delta) \\ \text{s.t.} \quad & \|\delta\|_p \leq q. \end{aligned} \tag{6}$$

The main problem here is that the constrained non-convex optimization is hard to solve. Though one can apply the projected gradient descent to ensure the solution is always feasible, unlike the box-constraint in the common L_∞ attacks, the projection operation is challenging under the complex L_1 and L_2 norm constraints. Thus, we propose the reparameterization tricks to transform the constrained optimization (6) to the equivalent unconstrained optimization by exploiting the property of L_1 and L_2 norms.

For the L_1 attack, we notice that the unit L_1 norm ball $\mathcal{B}_1 = \{\delta \in \mathbb{R}_{+,0}^n \mid \|\delta\|_1 = 1\}$ is the set of all n-dimensional probability distribution vectors. Thus, we can resolve the unit L_1 norm constraint in (6) with Softmax reparameterization as follows. Let $\mathbf{z} \in \mathbb{R}^n$ be the variable to reparameterize δ.

$$\delta_i = \frac{e^{z_i}}{\sum_{j=1}^{n} e^{z_j}} \quad \forall i \in [n]$$

To generalize it to the L_1 norm within $[0, q]$, we define $\mathbf{r} \in \mathbf{R}^n$ and reparameterize δ as follows

$$\delta_i = q \cdot \frac{(tanh(r_i) + 1) \cdot e^{z_i}}{2 \sum_{j=1}^{n} e^{z_j}} \quad \forall i \in [n] \tag{7}$$

One can easily verify that δ satisfies the L_1 norm constraint and every feasible δ can be reparameterized with suitable $\mathbf{r}$ and $\mathbf{z}$.

The L_2 norm constraint of δ can also be resolved with similar reparameterization trick using $\mathbf{r}$ and $\mathbf{z}$.

$$\delta_i = q \cdot \frac{(tanh(r_i) + 1) \cdot e^{z_i}}{2\sqrt{\sum_{j=1}^{n} e^{2z_j}}} \quad \forall i \in [n] \tag{8}$$

With reparameterization, we solve the following unconstrained optimization which is equivalent to (6).

$$\min_{\mathbf{r}, \mathbf{z} \in \mathbb{R}^n} \quad f^{\mathbf{w}}(\mathbf{x} + \delta) \tag{9}$$

where δ is in the forms of (7) and (8) for L_1 and L_2 attacks respectively.

We use the Adam optimizer to conduct gradient descent to solve (9). After the continuous solution δ is obtained, we round it into a discrete solution satisfying the L_p norm bound of q. The rounding process works as follows. We pick a threshold value η from $[0, 1]$. Let $\tilde{\delta}$ be the solution of (9). For each entry $\tilde{\delta}_i$, if the residual value $\tilde{\delta}_i - \lfloor \tilde{\delta}_i \rfloor$ is larger than η, we set δ_i be $\lfloor \tilde{\delta}_i \rfloor + 1$ and otherwise, δ_i is assigned with $\lfloor \tilde{\delta}_i \rfloor$. The binary search is conducted on possible threshold values and output the final solution δ such that no feasible δ with $\|\delta\|_p \le q$ can be obtained with higher threshold value. As there are at most n different residual values, the binary search can be done within $\log(n)$ rounds.

7 ADVERSARIAL TRAINING FOR IMPROVING ROBUSTNESS

In order to improve the robustness of the deep fraud detector, we incorporate adversarial examples into the training process (Algorithm 5), and solve the following robust optimization

$$\min_{\mathbf{w}} \mathop{\mathbb{E}}_{(\mathbf{x}, y) \sim \mathcal{D}} [\max_{\delta \in \Delta^1_{q_1} \cup \Delta^2_{q_2}} L^{\mathbf{w}}(\mathbf{x} + \delta, y)] \tag{10}$$

where we omit the regularization term. Adversarial training (Algorithm 5) is a common practice to solve (10). The idea is to incorporate the adversarial examples into the training process and to approximate the optimization of the inner problem in (10). Noticing that both L_1 and L_2 attacks are considered in this paper, at each iteration, for each fraud instance in minibatch $\mathcal{B}$ of training data, we uniformly pick p from $\{1, 2\}$ and generate one adversarial example with IFCM$_p$. All the generated adversarial examples are grouped into $\mathcal{B}^{adv}$, which is concatenated with $\mathcal{B}$ to form the new minibatch training data $\mathcal{B}'$. A training step is then conducted on $\mathcal{B}'$ with the following loss function

$$\begin{aligned} \tilde{L}^{\mathbf{w}}(\mathbf{x}, y) =& \mathbb{1}_{\{y=0\}} L^{\mathbf{w}}(\mathbf{x}, y) + (1 - \gamma) \mathbb{1}_{\{y=1\}} L^{\mathbf{w}}(\mathbf{x}, y) \\ &+ \gamma \mathbb{1}_{\{y=1\}} L^{\mathbf{w}}(\mathbf{x}^{adv}, y) \end{aligned} \tag{11}$$

where γ is the parameter balancing the loss of the original data and adversarial examples.

Algorithm 5: Adversarial training with IFCM

Randomly initialize the network for fraud detection;
repeat
  Read minibatch $\mathcal{B} \subset \mathcal{D}$ from training set $\mathcal{D}$;
  For each fraud instance in $\mathcal{B}$, randomly selects $p \in \{1, 2\}$ and create an adversarial example with IFCM$_p$, grouped into $\mathcal{B}^{adv}$;
  Concatenate $\mathcal{B}^{adv}$ with $\mathcal{B}$ as $\mathcal{B}'$;
  Conduct one training step over $\mathcal{B}'$ with loss $\tilde{L}$ in (11);
until training converged;

8 EXPERIMENTAL EVALUATION

In this section, we present extensive experimental evaluation to illustrate the performance of our methods.

8.1 Experimental Settings

8.1.1 Dataset and Data Analysis. Our dataset is provided by TaoBao, one of the largest e-commerce platforms in the world. The dataset contains all transaction data in a period of 30 days. Each transaction is encoded as a feature vector to represent its statistics and characteristics, including various prices, the number of historical purchases on an item, the offline metrics on fraudulent suspicious of the buyer and item, and the statistics on a user's preference, depicted by the records of interactions on all categories in the past one month. We randomly sample 1.5 million fraud transactions and 1.5 million benign instances from the data in the first 25 days to form a balanced training set. We uniformly pick 300 thousand transactions from the records of the last 5 days as the test data, where the proportion of fraud instances to benign ones is around 1 : 30.

We provide some statistics on the preference features to give a better impression on the fraud detection problem. One key statistic is the L_1 norm of a transaction instance $\mathbf{x}$, that is, the total number of interactions recorded in the past month. We notice that in the fraud transactions, 66.8% have zero interaction, i.e., $\|\mathbf{x}\|_1 = 0$[6], while the percentage is only 3.9% in the benign transactions. According to the explanation from domain experts in TaoBao, those fraud instances with zero L_1 norms are likely to be generated by large number of simple and cheap robots or scripts by the platforms, which are also easier to detect. The remaining fraud instances with non-zero L_1 norms correspond to the sophisticated scripts, such as the one in Figure 2, which makes complicated operations to behave like humans. Table 1 presents the distribution of $\|\mathbf{x}\|_1$ of instances with non-zero L_1 norms, as well as the mean value of $\|\mathbf{x}\|_1$.

There are several points we would like to make regarding these statistics. First, though it seems reasonable to have two separate classifiers, one for instances with zero L_1 norm and the other for the remaining instances, empirical attempts show that it provides

[6] We would like to remind the reader that for simplicity, we only consider the preference features to encode an instance, while in the deployed model, there are other non-zero features.

Type	$\|\mathbf{x}\|_1 \leq 100$	$100 < \|\mathbf{x}\|_1 \leq 200$	$200 < \|\mathbf{x}\|_1 \leq 300$	$\|\mathbf{x}\|_1 > 300$	mean($\|\mathbf{x}\|_1$)
fraud	33.87%	16.43%	10.85%	38.85%	**377**
benign	45.33%	23.56%	12.8%	18.31%	**208**

Table 1: Statistics on fraud and benign instances with non-zero L_1 norms

little improvement and brings extra vulnerability to adversarial attack. Thus, we use a single classifier as the detector for all instances. Second, despite the high amount of fraud instances with zero L_1 norms, the perturbation on those instances is meaningful as it indicates the potential that the adversary improves their simple bots with extra functions. Third, we also evaluate our attacks on fraud instances with non-zero L_1 norms separately, and the slight perturbation can still bypass the detector with high chance. For example, with $q = 20$ in L_1 attack, which corresponds to the distortion ratio of only around 5% given that the mean value of $\|\mathbf{x}\|_1$ is 377 for fraud instances with non-zero L_1 norms, the adversarial examples generated by AIS_1 can fool the detector with probability over 50%.

8.1.2 Model Training and Attack Settings. The deep fraud detector model is trained with the following parameters. The training batch size is 500 and the model is trained over 30000 batches. Adam [12] optimizer is used to conduct the stochastic gradient descent and the learning rate is set to be 0.0002. The regularization parameter α is set to be 0.01. The adversarial training is conducted with adversarial examples generated by IFCM_1 and IFCM_2, with $q = 30$ and $q = 6$ respectively. To test the attacking effectiveness of various algorithms, we consider $q \in \{10, 20, 30\}$ for the L_1 attack and $q \in \{4, 5, 6\}$ for the L_2 attack. In evaluation of the detector strengthened with adversarial training, we also try larger values of q, such as $q \in \{10, 20, 30, 40, 50\}$ for the L_1 attack and $q \in \{4, 5, 6, 7\}$ for the L_2 attack.

8.1.3 Baselines. We adapt several state-of-the-art continuous attacks to generate discrete perturbations, including FGSM [8], C&W attack [4], Logit-Space attack [2], and EAD attack [5].

FGM_1: FGM_1 is a single step L_1 attack method which selects the q coordinates with the minimal partial derivatives and adds one unit perturbation on each of them.

C&W attack: C&W attack is an optimization-based method primarily for continuous L_0, L_2, and L_∞ attacks on image classifiers. We adapt it to generate L_1 attack and use rounding techniques to obtain the discrete perturbation satisfying the norm constraint. C&W uses the Change of Variables (CoV) to replace δ with $\frac{q}{2}(tanh(\mathbf{w})+1)$ (element-wise) and solves the following continuous optimization

$$\min_{\mathbf{w}\in\mathbb{R}^n} c \cdot f(\mathbf{x} + \frac{q}{2}(tanh(\mathbf{w}) + 1)) + \|\frac{q}{2}(tanh(\mathbf{w}) + 1)\|_p$$

where $f(\mathbf{x}^{adv})$ is suggested to be defined as the difference of the logits, i.e., $f(\mathbf{x}^{adv}) = \max(z_1^{adv} - z_0^{adv}, 0)$ [4] with $\mathbf{z}^{adv}$ being the output of the last hidden-layer when the adversarial example $\mathbf{x}^{adv} = \mathbf{x} + \frac{q}{2}(tanh(\mathbf{w}) + 1)$ is the input. We replace it with $f(\mathbf{x}^{adv}) = z_1^{adv} - z_0^{adv}$ as z_1 tends to be larger than z_0 in our tested detector and the suitable threshold is around 0.9, rather than 0.5. Constant c is selected with binary search to ensure that $f(\mathbf{x}^{adv})$ is minimized to the extend while $\|\frac{q}{2}(tanh(\mathbf{w}) + 1)\|_p \leq q$ is still satisfied[7]. The optimization is solved with Adam optimizer. We pick the hyper-parameters that perform the best in solving the optimization in our tests, including the learning rate of 0.1 with 1000 gradient descent steps. 16 binary searches are conducted on $c \in [0, 100]$. The continuous solution δ is rounded off in a similar way as R3 attack. After the binary search returns the optimal c, we solve the optimization with 5 random starting-points of $\mathbf{w}$ and pick the best rounded discrete solution.

C&W-LS attack: Logit-Space attack [2] uses one-hot encoding to represent the discrete feature and applies the Softmax reparameterization to approximate the one-hot encoding. Formally, δ_i is represented by $Softmax(\mathbf{w}_i) \cdot (0, 1, ..., q)$ and the optimized variable is changed to $W = [\mathbf{w}_1, ..., \mathbf{w}_n]$. The optimization is similar to C&W attack, except that an entropy penalty is imposed to penalize δ_i being fractional. That is, C&W-LS solves the following optimization

$$\min_{W\in\mathbb{R}^{n\times(q+1)}} c\cdot f(\mathbf{x}+U(0, 1, ..., q)^T)+\|U(0, 1, ..., q)^T\|_p+\beta\cdot \sum_{i\in[n]} H(\mathbf{u}_i)$$

where $U = [\mathbf{u}_1, ..., \mathbf{u}_n]$, $\mathbf{u}_i = Softmax(\mathbf{w}_i)$, i.e., $u_{ij} = \frac{e^{w_{ij}}}{\sum_{j'=0}^{q} e^{w_{ij'}}}$ for $j \in \{0, 1, ..., q\}$, and $H(\mathbf{u}_i) = -\sum_{j=0}^{q} u_{ij} \log(U_{ij})$ is the entropy for $\mathbf{u}_i$ regarded as a distribution, which is minimized when $\mathbf{u}_i$ is one-hot. The implementation follows the same settings as C&W attack. We try different values of β and choose the best one in evaluation, which is 0.1 for L_1 attack and 0.5 for L_2 attack.

EAD attack: EAD attack [5] is a continuous L_1 attack on image classifier. It is also optimization-based attack which solves the following optimization problem with elastic-net regularization

$$\min_{\delta\in\mathbb{R}^n_{0,+}} c \cdot f(\mathbf{x} + \delta) + \beta \cdot \|\delta\|_1 + \|\delta\|_2^2$$

We try different values of β and choose the best one in evaluation, which is 5.0.

We also try to round other attack algorithms such as DeepFool [17] for discrete L_2 attack. However, since DeepFool aims to find the successful attack with the smallest L_2 distortion and thus imposes no norm restriction on perturbation. The rounding solution of DeepFool performs poorly. We also implement the random attack, which has little effect on degrading the performance of the classifier. Therefore, the results of these attempts are not presented in the paper.

8.1.4 Evaluation Metrics. We evaluate various attacks and adversarial training based on two metrics, *success rate* and *Average Precision (AP)*. Success rate measures the proportion of fraud instances which are correctly recognized by the detector with pre-defined threshold η and mis-classified under the attack. AP is commonly

[7]Though in [4], the binary search on c aims to ensure the minimal value of c such that δ successfully fools the detector, it performs worse than our implementation when rounding the solution to the discrete one with L_p norm bound q. Thus, we implement C&W attack in the way explained here.

Attack	Original model			Model with adversarial training				
	$q = 10$	$q = 20$	$q = 30$	$q = 10$	$q = 20$	$q = 30$	$q = 40$	$q = 50$
unattack	0.892	0.892	0.892	0.89	0.89	0.89	0.89	0.89
FGM_1	0.817	0.798	0.787	0.882	0.885	0.892	0.902	0.901
C&W	0.763	0.516	0.442	0.889	0.892	0.897	0.897	0.9
C&W-LS	0.765	0.572	0.575	0.889	0.889	0.889	0.885	0.887
EAD	0.767	0.573	0.393	0.887	0.891	0.895	0.896	0.896
$IFCM_1$	0.767	0.578	0.409	0.879	**0.876**	**0.875**	0.876	0.876
R3	0.745	0.463	0.251	0.881	0.877	**0.875**	**0.873**	**0.859**
AIS_1	**0.726**	**0.434**	**0.238**	**0.88**	**0.876**	**0.875**	0.874	0.873

Table 2: ***Average Precision (AP)*** **of the original model and the model with adversarial training under L_1 attacks**

Attack	Original model			Model with adversarial training			
	$q = 4$	$q = 5$	$q = 6$	$q = 4$	$q = 5$	$q = 6$	$q = 7$
unattack	0.892	0.892	0.892	0.89	0.89	0.89	0.89
C&W	0.71	0.492	0.238	0.882	0.889	0.893	0.887
C&W-LS	0.66	0.447	0.256	0.888	0.893	0.897	0.9
$IFCM_2$	0.66	0.485	0.343	**0.877**	**0.876**	0.876	0.877
R3	0.68	0.463	**0.205**	0.894	0.895	**0.875**	0.877
AIS_2	**0.57**	**0.344**	0.207	0.878	0.877	0.876	**0.875**

Table 3: ***Average Precision (AP)*** **of the original model and the model with adversarial training under L_2 attacks**

Attack	$\|\mathbf{x}\| = 0$			$\|\mathbf{x}\| > 0$		
	$q = 10$	$q = 20$	$q = 30$	$q = 10$	$q = 20$	$q = 30$
FGM_1	5.4%	11.1%	13.4%	22.4%	34.1%	41%
C&W	10.1%	73.4%	75.4%	25.9%	47.4%	53.6%
C&W-LS	9.6%	45.5%	58.7%	25.7%	43.6%	44.7%
EAD	9.7%	58.5%	76.5%	26.6%	49%	60.7%
$IFCM_1$	9.7%	58.4%	90.4%	26.3%	49.4%	64.6%
R3	14.1%	81.4%	97.6%	27.9%	53.4%	**66.5%**
AIS_1	**19.3%**	**84.9%**	**97.8%**	**28.7%**	**54.1%**	66.4%

Table 4: ***Success rate*** **of L_1 attacks**

Attack	$\|\mathbf{x}\| = 0$			$\|\mathbf{x}\| > 0$		
	$q = 4$	$q = 5$	$q = 6$	$q = 4$	$q = 5$	$q = 6$
C&W	21.7%	64.4%	94.3%	37%	55.3%	68.7%
C&W-LS	28.2%	82.7%	95.3%	39.3%	58.7%	68.3%
$IFCM_2$	23.7%	78.4%	96.5%	39.2%	58.4%	69.8%
R3	28.8%	72%	94.5%	37.3%	56%	69.9%
AIS_2	**59.7%**	**89.8%**	**98.7%**	**45%**	**61.4%**	**71%**

Table 5: ***Success rate*** **of L_2 attacks**

adopted to measure the performance of a classifier, which is defined by the enclosing area of the Precision-Recall curve (PR-curve). For a threshold η, the precision and recall are defined as follows [19]

$$P(\eta) = \frac{tp}{tp + fp} \quad R(\eta) = \frac{tp}{tp + fn},$$

where tp, fp and fn denote the true positive rate, false positive rate and false negative rate respectively. A higher value of AP intuitively means that the detector can recall a large proportion of fraud instances and meanwhile mis-classifies a few benign instances. A stronger attack should be able to degrade the AP to a lower value. The effectiveness of adversarial training can also be measured by AP by verifying whether the obtained model can pertain the AP under strong attacks. PR-curve is also useful for the selection of threshold in deployment. In practice, we choose the threshold η^* which equals the precision and recall, and we use η^* when evaluating the success rate of attacks. One thing to notice is that, an attack degrading the AP to a lower value doesn't mean it has higher success rate at η^*, since AP is an average measure of performance over all threshold values. We now present our key experimental results.

8.2 Average Precision

Tables 2 and 3 show the AP of the original detector and the one obtained via adversarial training under various L_1 and L_2 attacks respectively. Figure 3 shows the PR-curves of the detector under L_1 attacks with $q = 30$ and L_2 attacks with $q = 5$. We denote by *unattack* the trials without adversarial perturbation, corresponding to the performance on the original test data. The results show that (i) The deployed detector is extremely vulnerable to adversarial perturbations, as with $q = 20$ and $q = 5$ for AIS_1 and AIS_2 respectively, the AP is decreased from nearly 0.9 to 0.434 and 0.344. The numbers further decrease to 0.238 and 0.207 for AIS_1 attack with $q = 30$ and AIS_2 attack with $q = 6$ respectively. (ii) Our attack methods always achieve the largest degrade of AP in all settings, and significantly outperform baselines, especially AIS and R3, which show the similar performance. (iii) With adversarial training, the detector becomes significantly more robust to adversarial perturbations, as we consider larger q values 40, 50 for L_1 attack and 7 for L_2 attack, and the model can still achieve an AP above 0.859 in all

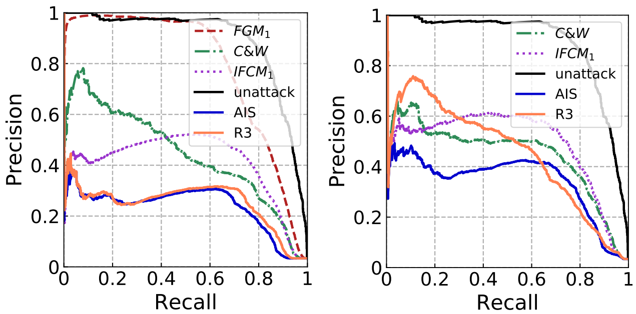

(a) L_1 attack, $q = 30$

(b) L_2 attack, $q = 5$

Figure 3: PR-curves.

Attack	L_1 attack			L_2 attack		
	$q = 10$	$q = 20$	$q = 30$	$q = 4$	$q = 5$	$q = 6$
FGM_1	0.005	0.005	0.005	-	-	-
IFCM	0.037	0.072	0.103	0.057	0.088	0.125
C&W	372.5	399.8	480.1	285.4	317.9	329.2
C&W-LS	290.1	313.6	455.9	299.5	301.3	333.2
EAD	71.8	87.4	89.5	-	-	-
R3	143.9	147.4	161.2	145.2	147.2	159.9
AIS	39.9	88.9	129.1	74.4	103.8	137.9

Table 6: Average runtime of generating one adversarial example (in seconds)

settings. Besides, the performance on the original test data is not degraded due to adversarial training, which shows the necessity of adversarial training[8].

8.3 Success Rate

Tables 4 and 5 show the success rates of tested L_1 and L_2 attacks respectively on the original model with threshold value η^*. To better understand the effectiveness of attacks, we separate the fraud instances based on the L_1 norm and randomly pick 1000 fraud instances with zero L_1 norm and 1000 fraud instances with non-zero L_1 norm. The results show that (i) Both types of fraud instances are highly vulnerable to adversarial perturbations. For instances with zero L_1 norm, with distortion bounds of 20 in L_1 norm and 5 in L_2 norm, our *AIS* attack can craft the instance to bypass the detector with probabilities over 84%. This shows the potential threat for the deployed system as the real-world adversaries and platforms may exploit this property and design more sophisticated scripts and bots with only tens of additional operations to bypass the detector with high changes. While for instances with non-zero L_1 norm, with distortion bounds of 20 in L_1 norm, which corresponds to an average distortion ratio of only 5% given the average L_1 norm for this type of instance being 377, our AIS_1 attack can fool the detector with probability 54.1%. (ii) Our attack methods achieve the highest success rates in all settings, and outperform baselines more significantly for instances with zero L_1 norm.

8.4 Feasibility of Attacks

8.4.1 Feasibility of Adversarial Perturbations. The perturbations generated here are not artificial noises on the input. Instead, there do exist such cases where the malicious service platform intentionally creates such perturbations. Recall that in the motivating scenario, we show an automatic script (Figure 2) by a malicious service provider. The script can conduct operations to pretend it as a human. One interesting pattern noticed by domain experts is that, when the script scrolls the item list on the website or mobile Apps, it will not directly visit the target item to create fake impression. Instead, it is designated with certain probability of visiting another item from certain categories and return to the item list. Imagine that fraudulent sellers and providers recognize the adversarial perturbations to bypass the detector. They can easily design effective scripts or even hire human labors to conduct the perturbation. Furthermore, we also sample adversarial perturbations and the domain experts verify that they are doable by the fraudulent sellers or malicious service providers.

8.4.2 Scalability of Attacks. Table 6 lists the average runtime of generating one adversarial example with various attacks. Notice that different attacks have varying proportions of computations able to be parallelized. Thus, the runtime of crafting a single instance cannot reflect the runtime of processing a batch of samples. From the adversary's perspective, our attacks are feasible as they can generate an adversarial examples within several minutes. Besides, one extra note on AIS is that it belongs to the *black-box* attacks as no information of the architecture of the detector is required. Thus, we argue that AIS could generate adversarial instances that are practical for real-world adversaries to craft.

[8]The proposed adversarial training process has been adopted to train the deep fraud detector for deployment since the Double 11 Shopping Festival of 2018.

9 CONCLUSION

This paper reveals the potential risk of deploying deep learning models in the task of fraud detection. We propose a fast attack called IFCM to generate large amount of effective adversarial examples, and two novel and more powerful attacks, search-based AIS attack and optimization-based R3 attack. We conduct extensive evaluations on a deployed deep fraud detector from TaoBao, one of the largest e-commerce platforms in the world with large-scale real-world transaction data. Results show that (i) Our proposed attacks can bypass the deployed detector with a high probability and can successfully degrade the Average Precision (AP) of the detector from nearly 90% to as low as 20% with slight perturbations. (ii) Our proposed attacks significantly outperform the state-of-the-art attack methods adapted to the domain of fraud detection, with respect to both the success rate and the degrading of AP of the detector in all testing trials. (iii) Our proposed adversarial training with the mixture of adversarial examples from both the L_1 and L_2 attacks significantly improves the robustness of the model, and pertains the AP of nearly 90% on the unperturbed test data.

ACKNOWLEDGMENTS

This research was supported by MOE, NRF, and NTU.

REFERENCES

[1] Anish Athalye, Nicholas Carlini, and David A. Wagner. 2018. Obfuscated Gradients Give a False Sense of Security: Circumventing Defenses to Adversarial Examples. In *Proceedings of the 35th International Conference on Machine Learning (ICML'18)*. 274–283.

[2] Jacob Buckman, Aurko Roy, Colin Raffel, and Ian Goodfellow. 2018. Thermometer Encoding: One Hot Way to Resist Adversarial Examples. (2018).

[3] Nicholas Carlini, Guy Katz, Clark Barrett, and David L Dill. 2017. Provably Minimally-Distorted Adversarial Examples. *arXiv* 1709 (2017).

[4] Nicholas Carlini and David A. Wagner. 2017. Towards Evaluating the Robustness of Neural Networks. In *2017 IEEE Symposium on Security and Privacy (SP'17)*. 39–57.

[5] Pin-Yu Chen, Yash Sharma, Huan Zhang, Jinfeng Yi, and Cho-Jui Hsieh. 2018. EAD: Elastic-Net Attacks to Deep Neural Networks via Adversarial Examples. In *Proceedings of the Thirty-Second AAAI Conference on Artificial Intelligence (AAAI'18)*. 10–17.

[6] Kang Fu, Dawei Cheng, Yi Tu, and Liqing Zhang. 2016. Credit Card Fraud Detection Using Convolutional Neural Networks. In *Neural Information Processing - 23rd International Conference (ICONIP'16)*. 483–490.

[7] Ian Goodfellow, Yoshua Bengio, Aaron Courville, and Yoshua Bengio. 2016. *Deep Learning*. Vol. 1.

[8] Ian J. Goodfellow, Jonathon Shlens, and Christian Szegedy. 2014. Explaining and Harnessing Adversarial Examples. *CoRR* abs/1412.6572 (2014).

[9] Kathrin Grosse, Nicolas Papernot, Praveen Manoharan, Michael Backes, and Patrick D. McDaniel. 2016. Adversarial Perturbations Against Deep Neural Networks for Malware Classification. *CoRR* abs/1606.04435 (2016).

[10] Geoffrey E. Hinton, Oriol Vinyals, and Jeffrey Dean. 2015. Distilling the Knowledge in a Neural Network. *CoRR* abs/1503.02531 (2015).

[11] Earlence Fernandes Tadayoshi Kohno Bo Li Atul Prakash Amir Rahmati Ivan Evtimov, Kevin Eykholt and Dawn Song. 2017. Robust Physical-World Attacks on Deep Learning Models. *arXiv preprint arXiv:1707.08945* (2017).

[12] Diederik P. Kingma and Jimmy Ba. 2014. Adam: A Method for Stochastic Optimization. *CoRR* abs/1412.6980 (2014).

[13] Alexey Kurakin, Ian J. Goodfellow, and Samy Bengio. 2016. Adversarial Examples in the Physical World. *CoRR* abs/1607.02533 (2016).

[14] Lingqiao Liu, Chunhua Shen, and Anton van den Hengel. 2015. The Treasure Beneath Convolutional Layers: Cross-Convolutional-Layer Pooling for Image Classification. In *IEEE Conference on Computer Vision and Pattern Recognition (CVPR'15)*. 4749–4757.

[15] Aleksander Madry, Aleksandar Makelov, Ludwig Schmidt, Dimitris Tsipras, and Adrian Vladu. 2017. Towards Deep Learning Models Resistant to Adversarial Attacks. *CoRR* abs/1706.06083 (2017).

[16] Seyed-Mohsen Moosavi-Dezfooli, Alhussein Fawzi, Omar Fawzi, and Pascal Frossard. 2017. Universal Adversarial Perturbations. In *2017 IEEE Conference on Computer Vision and Pattern Recognition (CVPR'17)*. 86–94.

[17] Seyed-Mohsen Moosavi-Dezfooli, Alhussein Fawzi, and Pascal Frossard. 2016. DeepFool: A Simple and Accurate Method to Fool Deep Neural Networks. In *2016 IEEE Conference on Computer Vision and Pattern Recognition (CVPR'16)*. 2574–2582.

[18] Vinod Nair and Geoffrey E. Hinton. 2010. Rectified Linear Units Improve Restricted Boltzmann Machines. In *Proceedings of the 27th International Conference on Machine Learning (ICML'10)*. 807–814.

[19] David L Olson and Dursun Delen. 2008. *Advanced Data Mining Techniques*.

[20] Nicolas Papernot and Patrick D. McDaniel. 2016. On the Effectiveness of Defensive Distillation. *CoRR* abs/1607.05113 (2016).

[21] Nicolas Papernot, Patrick D. McDaniel, Somesh Jha, Matt Fredrikson, Z. Berkay Celik, and Ananthram Swami. 2016. The Limitations of Deep Learning in Adversarial Settings. In *IEEE European Symposium on Security and Privacy (EuroS&P'16)*. 372–387.

[22] Nicolas Papernot, Patrick D. McDaniel, Xi Wu, Somesh Jha, and Ananthram Swami. 2016. Distillation as a Defense to Adversarial Perturbations Against Deep Neural Networks. In *IEEE Symposium on Security and Privacy (SP'16)*. 582–597.

[23] Herbert Robbins and Sutton Monro. 1985. A stochastic approximation method. In *Herbert Robbins Selected Papers*. 102–109.

[24] Andrew Slavin Ross and Finale Doshi-Velez. 2018. Improving the Adversarial Robustness and Interpretability of Deep Neural Networks by Regularizing Their Input Gradients. In *Proceedings of the Thirty-Second AAAI Conference on Artificial Intelligence (AAAI'18)*. 1660–1669.

[25] Mahmood Sharif, Sruti Bhagavatula, Lujo Bauer, and Michael K. Reiter. 2016. Accessorize to a Crime: Real and Stealthy Attacks on State-of-the-Art Face Recognition. In *Proceedings of the 2016 ACM SIGSAC Conference on Computer and Communications Security (CCS'16)*. 1528–1540.

[26] Ning Su, Yiqun Liu, Zhao Li, Yuli Liu, Min Zhang, and Shaoping Ma. 2018. Detecting Crowdturfing "Add to Favorites" Activities in Online Shopping. In *Proceedings of the 2018 World Wide Web Conference on World Wide Web (WWW'18)*. 1673–1682.

[27] Christian Szegedy, Wojciech Zaremba, Ilya Sutskever, Joan Bruna, Dumitru Erhan, Ian J. Goodfellow, and Rob Fergus. 2013. Intriguing Properties of Neural Networks. *CoRR* abs/1312.6199 (2013).

[28] Florian Tramèr, Alexey Kurakin, Nicolas Papernot, Dan Boneh, and Patrick D. McDaniel. 2017. Ensemble Adversarial Training: Attacks and Defenses. *CoRR* abs/1705.07204 (2017).

[29] Haiqin Weng, Zhao Li, Shouling Ji, Chen Chu, Haifeng Lu, Tianyu Du, and Qinming He. 2018. Online E-Commerce Fraud: A Large-Scale Detection and Analysis. In *34th IEEE International Conference on Data Engineering (ICDE'18)*.

[30] Weilin Xu, David Evans, and Yanjun Qi. 2018. Feature Squeezing: Detecting Adversarial Examples in Deep Neural Networks. In *25th Annual Network and Distributed System Security Symposium (NDSS'18)*.

[31] Xiaoyong Yuan, Pan He, Qile Zhu, Rajendra Rana Bhat, and Xiaolin Li. 2017. Adversarial Examples: Attacks and Defenses for Deep Learning. *CoRR* abs/1712.07107 (2017).

[32] Ashkan Zakaryazad and Ekrem Duman. 2016. A Profit-Driven Artificial Neural Network (ANN) with Applications to Fraud Detection and Direct Marketing. *Neurocomputing* 175 (2016), 121–131.

[33] Mengchen Zhao, Zhao Li, Bo An, Haifeng Lu, Yifan Yang, and Chen Chu. 2018. Impression Allocation for Combating Fraud in E-commerce Via Deep Reinforcement Learning with Action Norm Penalty. In *Proceedings of the Twenty-Seventh International Joint Conference on Artificial Intelligence (IJCAI'18)*. 3940–3946.

[34] Panpan Zheng, Shuhan Yuan, Xintao Wu, Jun Li, and Aidong Lu. 2018. One-Class Adversarial Nets for Fraud Detection. *CoRR* abs/1803.01798 (2018).

[35] Stephan Zheng, Yang Song, Thomas Leung, and Ian J. Goodfellow. 2016. Improving the Robustness of Deep Neural Networks via Stability Training. In *2016 IEEE Conference on Computer Vision and Pattern Recognition (CVPR'16)*. 4480–4488.